BIOCHEMISTRY
including biophysical chemistry & molecular biology
Article

Biochemistry **2010,** *49,* 8307–8315 8307
DOI: 10.1021/bi100968m

Activation and Specificity of Human Caspase-10[†]

Katherine Wachmann,[‡,∥] Cristina Pop,[‡] Bram J. van Raam,[‡] Marcin Drag,[‡,⊥] Peter D. Mace,[‡] Scott J. Snipas,[‡] Christian Zmasek,[§] Robert Schwarzenbacher,[∥] Guy S. Salvesen,[‡] and Stefan J. Riedl*[,‡]

[‡]*Program in Apoptosis and Cell Death Research, and* [§]*Program for Bioinformatics and Systems Biology, Sanford-Burnham Medical Research Institute, 10901 North Torrey Pines Road, La Jolla, California 92037,* [∥]*Department of Molecular Biology, University of Salzburg, 5020 Salzburg, Austria, and* [⊥]*Division of Medicinal Chemistry and Microbiology, Faculty of Chemistry, Wroclaw University of Technology, Wybrzeze Wyspianskiego 27, 50-370 Wroclaw, Poland*

Received June 15, 2010; Revised Manuscript Received August 4, 2010

ABSTRACT: Two apical caspases, caspase-8 and -10, are involved in the extrinsic death receptor pathway in humans, but it is mainly caspase-8 in its apoptotic and nonapoptotic functions that has been an intense research focus. In this study we concentrate on caspase-10, its mechanism of activation, and the role of the intersubunit cleavage. Our data obtained through *in vitro* dimerization assays strongly suggest that caspase-10 follows the proximity-induced dimerization model for apical caspases. Furthermore, we compare the specificity and activity of the wild-type protease with a mutant incapable of autoprocessing by using positional scanning substrate analysis and cleavage of natural protein substrates. These experiments reveal a striking difference between the wild type and the mutant, leading us to hypothesize that the single chain enzyme has restricted activity on most proteins but high activity on the proapoptotic protein Bid, potentially supporting a prodeath role for both cleaved and uncleaved caspase-10.

Apoptosis is a form of programmed cell death that requires members of a family of aspartate-specific cysteine proteases, called caspases, to both initiate and execute the apoptotic phenotype (*1*, *2*). They can be subdivided into apical (caspase-8,-9, and -10) and effector caspases (caspase-3, -6, and -7). When a death signal triggers an apoptotic pathway, apical caspases are activated and are then able to activate effector caspases by proteolytic cleavage, leading to cell death. There are two main pathways responsible for apoptosis: the extrinsic pathway, which is activated through ligation of death receptors and involves caspase-8 and-10, and the intrinsic mitochondrial pathway involving caspase-9 (*3*−*6*). Apical caspases carry a large N-terminal prodomain (DED,[1] death effector domain, in caspase-8 and -10, and CARD, caspase-recruitment domain, in caspase-9) followed by the catalytic domain composed of a large and small subunit separated by a linker region (*2*, *7*).

Upon a death stimulus, apical caspases, which are expressed as latent monomeric zymogens, are recruited to a polymeric activation complex that enables them to generate proteolytic activity. For both caspase-8 and caspase-10 this platform is known as the death-inducing signaling complex (DISC). The best characterized DISC consists of the death receptor Fas, FADD (Fas-associated death domain protein) and the apical caspase which interacts with FADD via homophilic interactions of DEDs (*8*−*11*). Besides caspase-8 and -10, the catalytically inactive homologue of caspase-8, cFLIP, has been found to be present at the DISC (*12*, *13*) and has been shown to enhance caspase-8 activity forming heterodimers with the enzyme (*14*). The DISC provides a platform for zymogen dimerization with subsequent autocatalytic cleavage in the intersubunit linker between their large and small chains, leading to what is known as proximity-induced activation (*15*). In this model dimerization is the required event for activation, and proteolysis in the intersubunit linker is an important stabilizing event that promotes apoptotic potential (*16*−*20*).

In vitro, dimerization can be induced by kosmotropic salts such as sodium citrate (*15*) or by introducing hybrids of caspase-8 with synthetic N-terminal dimerization domains that dimerize upon addition of a tight binding compound (*21*, *22*). Human caspase-10 and caspase-8 are highly homologous in their protein sequence (46% identical in the catalytic domain), and their genes are on the same region of human chromosome 2q33-34 (*23*−*25*), suggesting that they have a common ancestor. For caspase-10, at least seven splice variants have been identified on the mRNA level (caspase-10 a-f) (*26*−*29*), of which some are truncated and lack the catalytic subunits while others vary in their C-termini.

It has long been assumed that caspase-8 and caspase-10 are redundant in their functions, and there is controversy in the literature on whether caspase-10 can functionally substitute for caspase-8 in mediating death-receptor-dependent cell death (*27*, *30*, *31*). Caspase-10 has been deleted from the genome in the rodent lineage, which may be the main factor for the heavy focus on caspase-8 over caspase-10 in the literature. However, there is emerging research showing that caspase-10 is equally

[†]This work is supported by NIH grant R01AA017238 to S.J.R., EC Grant MCEXT033534 to R.S., and NIH Grant CA69381 to G.S.S. M.D. is supported by the Foundation for Polish Science. B.J.v.R. is supported by the Rubicon fellowship from The Netherlands Organization for Scientific Research (NWO).

*To whom correspondence should be addressed. Phone: (858) 646-3100. Fax: (858) 646-3199. E-mail: sriedl@sanfordburnham.org.

[1]Abbreviations: DED, death effector domain; CARD, caspase recruitment domain; DISC, death-inducing signaling complex; FADD, Fas-associated death domain protein; cFLIP, cellular FLICE-like inhibitory protein; FasL, Fas ligand; ALPS, autoimmune lymphoproliferative syndrome; Fv-domain, FK506 binding protein (FKBP) with Phe36Val; z-VAD-FMK, carbobenzoxy-Val-Ala-Asp-fluoromethyl ketone; RIPK1, receptor-interacting serine/threonine-protein kinase 1; Ac-IETD-AFC, *N*-acetyl-Ile-Glu-Thr-Asp-(7-amino-4-trifluoromethylcoumarin); Ac-DEVD-AFC, *N*-acetyl-Asp-Glu-Val-Asp-(7-amino-4-trifluoromethylcoumarin); Ac-LEHD-AFC, *N*-acetyl-Leu-Glu-His-Asp-(7-amino-4-trifluoromethylcoumarin); c-10 WT, ΔDED two-chain caspase-10; c-10 D/A, ΔDED single-chain caspase-10.

Published on Web 08/26/2010

important, at least in its apoptotic functions. Caspase-10 mutations in humans combined with mutations in Fas and FasL have been associated with an autoimmune lymphoproliferative syndrome (ALPS) caused by defective lymphocyte apoptosis (*32*, *33*), and a function of this caspase in the intrinsic pathway has been proposed by several groups (*34*−*36*). Some studies have addressed the question of substrate specificity differences for caspase-8 and caspase-10 (*37*−*40*), but there is no thorough *in vitro* dissection of the inherent differences, activation mechanism, or importance of interdomain proteolysis of caspase-10. In this study we use an array of assays including hybrids of caspase-10 with synthetic N-terminal dimerization domains to unravel specific features of this apical caspase. Our results provide for the first time comprehensive insights into the question of whether caspases-8 and -10 are biochemically redundant in terms of their activity, activation mechanism, and substrate specificity.

MATERIALS AND METHODS

Recombinant Protein Expression and Purification. ΔDED caspase-10, isoform b (UniProt Q92851 lacking the first 202 residues), was subcloned into the *Nde*I and *Bam*HI sites of pET-15b, providing an N-terminal His_6 tag. Cleavage site mutant of ΔDED caspase-10 was generated by Asp/Ala substitution at $IEAD^{297}$. ΔDED caspase-10 and the ΔDED caspase-10 D297A were cloned into a pET-28b vector containing an FKBP-domain. Fv-domain, originating from a pC4-Fv1E expression vector (ARIAD Pharmaceuticals, Inc.), is a FK506 binding protein (FKBP) domain with a single amino acid substitution (Phe36Val) that binds with subnanomolar affinity to the synthetic FK506 derivate AP20187 (*21*, *22*). The final construct was a chimeric protein with an N-terminal His tag followed by the Fv-domain and the ΔDED caspase-10 and ΔDED caspase-10 D297A, respectively.

Expression and purification of caspases were carried out as described previously (*41*). Purified proteins were visualized on an 8%−18% SDS−PAGE gel by GelCode Blue staining.

Proteases were quantified by active site titration with z-VAD-fmk as previously described (*42*). Fv-caspase-10 was expressed and purified like the other caspases. Following the elution from Ni beads the protein was further purified by size-exclusion chromatography using a Superdex 200 column with an AKTA LC system (Pharmacia). The running buffer contained 50 mM Tris and 100 mM NaCl (pH 8.0).

Full-length mouse Bid containing an N-terminal 6×His in pET 21 (a kind gift from Dr. John Reed and Dr. Dayong Zhai (Sanford-Burnham Medical Research Institute) was expressed in *Escherichia coli* BL21 (DE3) by induction with 0.4 mM IPTG at 30 °C for 4 h and then purified by Ni^{+}-affinity chromatography, essentially as described for caspase expression and purification (*41*). FLAG-RIPK1 in pcDNA3 was a kind gift from Dr. Jurg Tschopp (University of Lausanne). The recombinant RIPK1 was transiently expressed in HEK293A cells and purified using M2 anti-FLAG beads (Sigma) as described for FLAG-tagged HDAC7 (*43*).

N-Terminal Sequencing of Protein Samples. Proteins were resolved by SDS−PAGE and transferred to PVDF membrane by electroblotting. The appropriate bands were cut after staining the membrane with Coomassie Brilliant Blue and subjected to Edman degradation using an ABI Procise 492.

Homology Modeling of Caspase-10. A structural model of caspase-10 was created based on the structure of pro-caspase-8 (PDB 2K7Z (*44*)) using MODELLER (*45*).

Size-Exclusion Chromatography. Fusion proteins were incubated for 30 min at 25 °C in standard caspase assay buffer with and without the dimerizer AP20187 at 1:1 ratio prior to injection onto a Superdex 200 column on an AKTA LC system (Pharmacia) in 50 mM Tris and 100 mM NaCl buffer, pH 7.4. The column was calibrated using gel filtration standard from Bio-Rad.

Sodium Citrate Titration. Caspase-10 (10 nM) was incubated with a dilution series of sodium citrate buffer for 30 min at 37 °C. The stock sodium citrate buffer contains 1.6 M sodium citrate, 20 mM PIPES, and 100 mM NaCl, pH 7.4. Standard caspase assay buffer contains 20 mM PIPES, 100 mM NaCl, 10% sucrose, 10 mM DTT, and 0.05% CHAPS, pH 7.4. Activity was measured by adding the substrate Ac-IETD-AFC (100 μM) and detecting emission at 510 nm on excitation at 405 nm on a Molecular Device fmax-plate reader at 37 °C.

For titration in the presence of dimerizer AP20187 the protease (30 nM) was incubated with the compound at 1:1 ratio for 30 min at 25 °C. Sodium citrate buffer was added, and the mix was incubated for another 30 min at 25 °C before monitoring substrate hydrolysis (Ac-IETD-AFC, 100 μM) at 30 °C.

Titration with Dimerizer AP20187. Fv-caspase-10 (30 nM) was prepared in standard caspase assay buffer and incubated with a dilution series of AP20187 at 25 °C for 30 min. Ac-IETD-AFC was added (100 μM) for monitoring activity at 30 °C. Activity in 1 M citrate buffer was used as a positive control.

Positional Scanning Library. Positional scanning substrate combinatorial library (PS-SCL) was synthesized as described earlier (*46*). Proteins were preincubated in 1 M sodium citrate buffer for 15 min at 37 °C before they were added to the substrate library at final concentration of 5 nM for caspase-10 wild type and 50 nM for caspase-10 cleavage site mutant. Analyses of the results were based on total RFUs (relative fluorescence units) converted to percent maximum activity with the highest value set to 100%.

Caspase-10 Catalytic Parameters. The catalytic parameters k_{cat} and K_M were determined by measuring substrate hydrolysis upon adding 10 nM protease to a dilution series ranging from 1 μM to 1 mM of peptide substrates (Ac-DEVD-AFC, Ac-IETD-AFC, and Ac-LEHD-AFC). Proteins were preincubated in 1 M sodium citrate buffer for 30 min at 37 °C. Since substrate saturation could not be reached with Ac-DEVD-AFC for the cleavage site mutant, we could not determine separate k_{cat} and K_M values, but with the assumption that the reaction follows Michaelis−Menten kinetics, we applied the following equation with $[S] \ll K_M$ (eq 1) for estimating k_{cat}/K_M:

$$v = \frac{k_{cat}[E][S]}{K_M} \quad (1)$$

[E] is the concentration of enzyme, [S] is the concentration of substrate, and v is the initial velocity.

Protein Cleavage Kinetics. Protein substrates (1 μM) were incubated with a dilution series of caspase-10 wild type or cleavage site mutant for 1 h at 37 °C. The enzymes were preincubated in 1 M sodium citrate buffer for 30 min at 37 °C. The reaction was terminated by adding 1 × SDS loading buffer and boiling of the samples. SDS−PAGE was performed followed by Western blot. Therefore, samples were transferred to PDVF membrane after electrophoresis. Membranes were blocked in 1% (w/v) Blotto dry-milk (Rockland) in TBS-T (20 mM Tris, pH 7.6, 137 mM NaCl with 0.2% (v/v) Tween 20) for 1 h, immunoblotted with

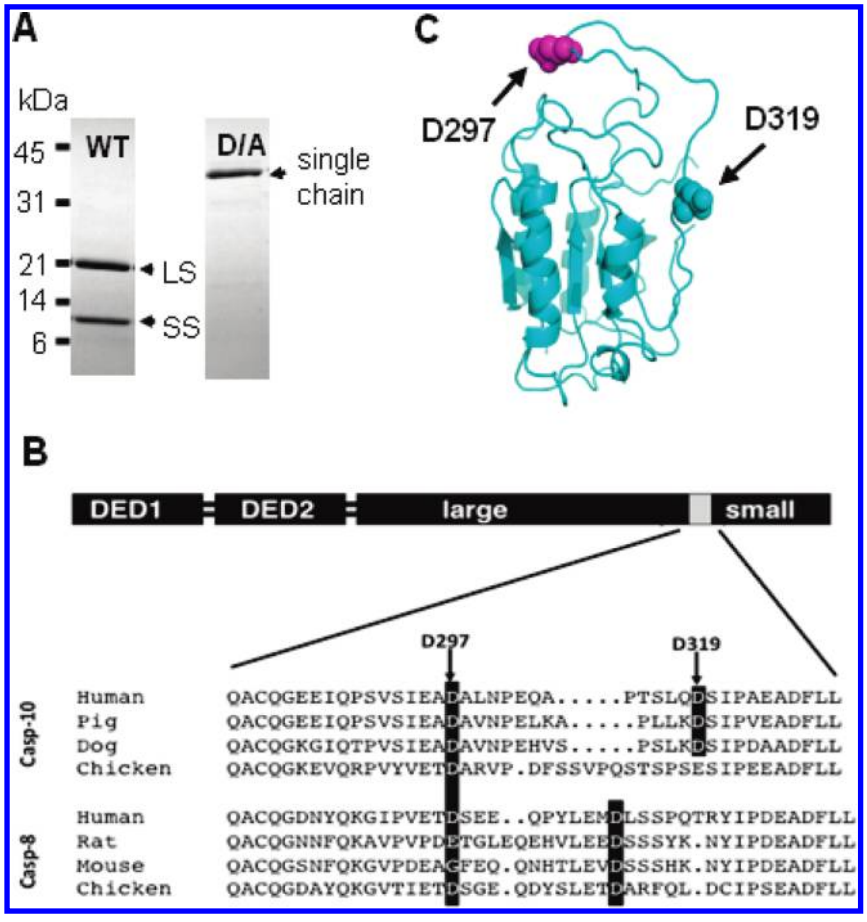

FIGURE 1: (A) SDS−PAGE of caspase-10 purification. Proteins were expressed in *E. coli*, purified by affinity chromatography, and visualized on an SDS−PAGE gel. The wild-type enzyme is autocleaved into large (LS) and small subunits (SS) during expression in *E. coli*. The cleavage site mutant D297A remains as a single chain of 35 kDa. (B) Structural organization and sequence alignment of caspase-8 and caspase-10 from various organisms. Numbering is according to the caspase-1 numbering convention. Putative conserved cleavage sites between the large and small subunit are highlighted. Caspase-10 has been deleted in the rodent lineage. (C) Model of pro-caspase-10 showing the potential cleavage sites between the large and small subunit. Pro-caspase-10 is autocatalytically processed into large and small subunits. The model shows the two conserved potential cleavage sites at D297 (magenta) and D319 (cyan). In this model D297 is presented as an extended loop, whereas D319 seems to be closer to the core of the monomer (modeled on caspase-8 zymogen, PDB 2K7Z).

primary antibody overnight at 4 °C in TBS-T, washed for 1 h in TBS-T, probed with anti-mouse (IR Dye 680; LI-COR Biosciences) or anti-rabbit (IR Dye 800CW, LI-COR Biosciences) secondary antibody for 1 h at room temperature, washed for 1 h with TBS-T, and analyzed on an Odyssey infrared scanner (LI-COR Biosciences). Densitometry was performed by quantifying the fluorescence signal. Densitometry was used to find $E_{1/2}$ which represents the concentration of protease that cleaves 50% of the full-length substrate in time (t). We then could determine k_{cat}/K_M using the half-life equation (eq 2):

$$\frac{k_{cat}}{K_M} = \frac{\ln 2}{tE_{1/2}} \quad (2)$$

Antibodies used were mouse monoclonal anti-caspase-3 (BD Transduction), mouse monoclonal anti-caspase-7 (Pharmingen), mouse monoclonal anti-RIPK1 (BD Transduction), and rabbit anti-Bid, which was a kind gift from Stan Krajewski (Sanford-Burnham Medical Research Institute).

RESULTS

Conventions and Definitions. Throughout the paper the caspase-1 numbering convention is used to simplify comparison with other caspases. All recombinant caspase-10 constructs were expressed without their DEDs, and for simplicity the ΔDED prefix is omitted in the remaining text.

Conserved Cleavage Sites in Caspase-10. Caspase-8, the close paralogue of human caspase-10, is expressed as a latent monomeric pro-caspase and is activated by proximity-induced dimerization. Dimerization is both necessary and sufficient for activation, whereas intersubunit cleavage is primarily a dimer stabilizing event (*15*). Expression and purification of caspase-10 from *E. coli* resulted in autoprocessing (Figure 1A). As expected, the wild-type enzyme displayed two bands on the gel representing the large (21 kDa) and small (10 kDa) subunits. N-Terminal sequencing of the small subunit confirmed cleavage at D297. To investigate the relevance of autoproteolysis in caspase-10, we generated the cleavage site mutant D297A. The wild type and the cleavage site mutant were purified by affinity chromatography and visualized on an SDS−PAGE gel (Figure 1A). Although there is a second conserved potential cleavage site at D319 (Figure 1B), the single mutation D297A completely abrogated autocleavage between the subunits, and the purified mutant was a single chain of 35 kDa. Structurally, this is most likely rooted in the fact that D319 resides proximal to the folded core structure of the caspase, making it inaccessible for efficient cleavage. In contrast, caspase-8, which has a longer linker than caspase-10 containing two well-exposed cleavage sites, undergoes proteolysis

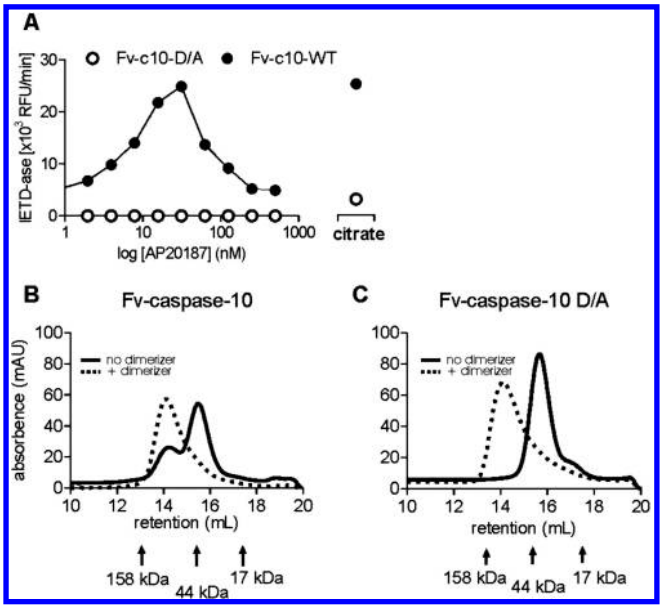

FIGURE 2: (A) Titration with dimerizer AP20187 induces activity of the wild type but not the cleavage site mutant. Fusion proteins (30 nM) were incubated with a dilution series of the dimerizer AP20187 in the absence of sodium citrate for 30 min at room temperature prior to adding Ac-IETD-AFC (100 μM). Activity in 1.0 M sodium citrate was used as a positive control (right). (B, C) The compound AP20187 dimerizes Fv-caspase-10. The enzyme was incubated with dimerizer for 30 min at 25 °C before performing size-exclusion chromatography. The fusion proteins run at their monomeric mass in the absence of AP20187 (full line). The Fv-caspase-10 (B) consists of a mixture of monomeric and dimeric species in the absence of AP20187. Upon addition of the compound all proteins run according to their dimeric mass (dotted line).

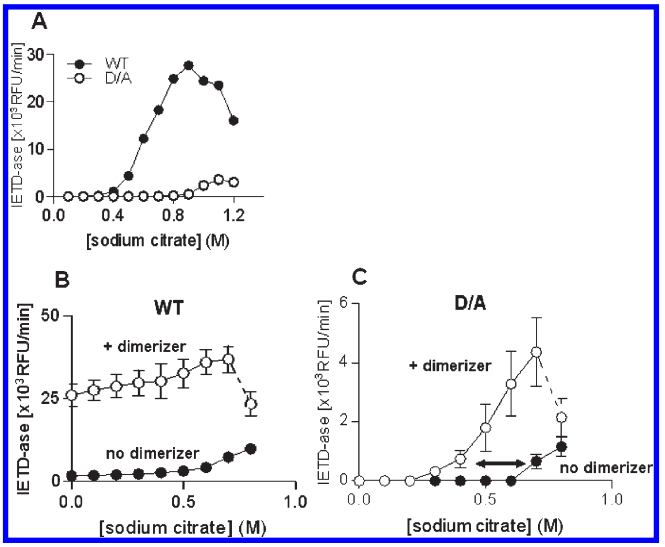

FIGURE 3: (A) Caspase-10 activation in sodium citrate. Caspase-10 (10 nM) wild type or cleavage site mutant was incubated with a dilution series of sodium citrate buffer for 30 min at 37 °C before monitoring activity by hydrolysis of Ac-IETD-AFC (100 μM). (B, C) Dimerization induced by AP20187 enhances overall activity of caspase-10. Protease (30 nM) was incubated with dimerizer (open circles) and without dimerizer (closed circles) at an optimal ratio for 30 min at room temperature. Sodium citrate buffer was added, and the mix was incubated for another 30 min at room temperature before monitoring substrate hydrolysis of Ac-IETD-AFC (100 μM). The activity of the wild type (B) was enhanced about 30% in the presence of dimerizer AP20187. The mutant (C) required less kosmotropic salt to gain activity indicated by the arrow in the figure. Experiments were repeated three times and data presented as mean ± standard deviation.

at both sites in the intersubunit linker, and mutation of both sites is required to prevent autoproteolysis (*17*). Curiously, another difference is observed in the linker at tyrosine residue 303, which has recently been implicated in regulation of caspase-8 via phosphorylation but is not conserved in caspase-10 (*47*). Because there is no atomic resolution structure of caspase-10, we generated a theoretical model (Figure 1C), using human caspase-8 as a template (*44*). On the basis of this model, even though the sequence surrounding D319 is compatible for cleavage by caspase-10, its location close to the compact core makes it unavailable for cleavage.

Chemically Inducible Dimerization Fusions Activate the Wild-Type but Not the Cleavage Site Mutant Caspase-10. To test whether homodimerization can directly activate caspase-10, we generated fusion proteins comprised of an N-terminal Fv-domain followed by the catalytic domain of the protease. The Fv-domain is a derivative of the FK506 binding protein (FKBP) (*21*) that dimerizes in the presence of the tight binding compound AP20187 (dimerizer), a derivative of rapamycin (*22*). The K_D of interaction of the compound with the Fv-domain is in the subnanomolar range (*21*, *22*); therefore, to ensure that we worked above the K_D, we chose a protein concentration of 30 nM. In this way, dimerization can be induced in a controlled manner. Titration with the dimerizer showed that optimal activation of the wild-type fusion protein occurs at a caspase to compound ratio of 1:1 (Figure 2A). To confirm that the compound AP20187 is indeed inducing dimerization, we subjected samples to size-exclusion chromatography and compared the theoretical molecular weights of monomer and dimer (Figure 2B,C). Note that the wild-type sample consists of a mixture of monomeric and dimeric species, typical of recombinant apical caspases (*15*, *20*). Upon addition of AP20187 all protein shifts to the dimeric form. At optimal compound concentration the activity of the wild-type protein was comparable to the activity induced by sodium citrate. Importantly, the D297A cleavage site mutant did not show any activity upon addition of the compound, suggesting that dimerization of the single-chain caspase by the Fv-domain is insufficient for activation (Figure 2A). However, we observed catalytic activity of the cleavage site mutant in sodium citrate, suggesting that sodium citrate enhances activity by a mechanism that goes beyond simple dimerization (see below).

Effects of Sodium Citrate on Caspase-10. This finding suggests that the action of citrate includes (i) dimer stabilization as reported previously (*15*) and (ii) organization of the active site, as expected from a kosmotrope that stabilizes compact arrangements of and in proteins (*48*).

In order to delineate the activation mechanism of caspase-10 and the effects of sodium citrate *per se*, we incubated the wild-type caspase or the cleavage site mutant with increasing amounts of the kosmotrope (Figure 3A). Enhanced activity was observed with increasing concentrations of kosmotrope, with about 100-fold activation for the D/A mutant and about 500-fold activation for the wild-type caspase-10. Interestingly, the cleavage site mutant showed only about 12% of the activity of the wild-type caspase-10 under optimal kosmotrope concentrations. The drop in activity of the wild type at 1.2 M sodium citrate is probably due to precipitation of the protein at this high salt concentration. In order to ensure robust activity for both caspase-10 wild type and the cleavage site mutant, we decided to use 1.0 M sodium citrate for all of the following experiments unless otherwise noted. Overall, the

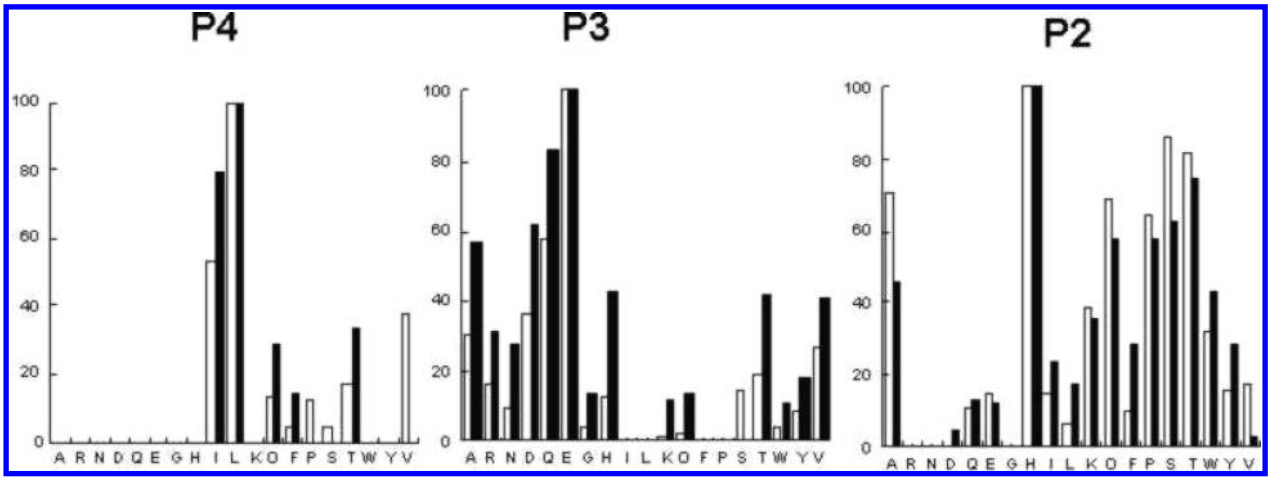

FIGURE 4: Cleaved and noncleavable caspase-10 reveal similar subsite preferences. Wild-type (cleaved) caspase-10 (black bars) and noncleavable caspase-10 (white bars) were tested on a P1 Asp-fixed positional scanning substrate library in the presence of 1.0 M sodium citrate. The *y*-axis represents the rate of hydrolysis as a percentage of the maximum measured rate. The *x*-axis shows the tested amino acids in single letter code, with norleucine (O) substituting for methionine.

results are consistent with the hypothesis of proximity-induced activation.

It has been hypothesized that sodium citrate promotes activation by dimerization but by being a kosmotrope also bears the ability to additionally stabilize loop regions important for activity. To test this hypothesis and to elucidate the role of dimerization in caspase-10 activation, we further analyzed the combined effects of the dimerizer AP20187 and the kosmotrope by performing a sodium citrate titration in the absence and presence of the dimerizer. Due to a loss of activity for the caspases in the presence of dimerizer above 0.8 M sodium citrate, we used this concentration as the upper limit for the titrations.

For the wild type, which was dimerized using AP20187, the kosmotrope had a minimal additional effect on activity (Figure 3B). The cleavage site mutant on the other hand required kosmotrope in addition to the dimerizer AP20187 for activity (Figure 3C). However and importantly, the dimerizer substantially lowered the concentration required to obtain activation, supporting the hypothesis that dimerization is the activating event and that other secondary events help to stabilize the dimer (Figure 3C). Both panels A and C of Figure 3 show close to no activity for the D/A mutant below 0.7 M kosmotrope while in the presence of dimerizer (Figure 3C) 50% of the maximal activity of caspase-10 D/A can be observed.

The decrease at 0.8 M sodium citrate in both titrations can be explained by partial misfolding or precipitation of the Fv-fusion protein at higher salt concentrations.

Cleaved and Noncleavable Caspase-10 Show Similar Subsite Preferences. To investigate whether cleavage of caspase-10 altered its substrate specificity, we profiled the wild type and mutant with a positional scanning substrate library, with P1 fixed as Asp, which explores preferences in the S2, S3, and S4 subsites, as previously described (*15*, *49*). The experiment was carried out in the presence of 1 M sodium citrate to ensure robust activity and revealed similar subsite preferences for both proteins. Both forms showed a somewhat restricted specificity in P4 but tolerated a wider range of residues in P3 and P2 (Figure 4). This restricted P4 preference is in stark contrast to caspase-8, which has been shown previously to have a broad acceptance of residues in P4 (*14*, *15*, *20*). Overall, our data reveal a similar subsite preference for caspase-10 wild type and cleavage site mutant but reduced activity for the mutant. To explore the basis for this reduced activity, we

Table 1: Catalytic Parameters on Different Peptide Substrates[a]

substrate	c-10	K_M (μM)	k_{cat} (s^{-1})	k_{cat}/K_M (M^{-1} s^{-1})
Ac-DEVD-AFC	WT	17 ± 0.7	0.66 ± 0.01	3.9×10^4
	D/A	nd	nd	1.1×10^3
Ac-LEHD-AFC	WT	15.7 ± 2.3	3.31 ± 0.11	2.1×10^5
	D/A	550 ± 42	7.96 ± 0.3	1.4×10^4
Ac-IETD-AFC	WT	8.4 ± 0.3	1.71 ± 0.02	2.0×10^5
	D/A	474 ± 42	7.82 ± 0.33	1.6×10^4

[a]Enzymes (10 nM) were incubated in 1.0 M sodium citrate for 30 min at 37 °C before measuring activity in a dilution series of the indicated substrates. Kinetic values (for three replicate data sets) were calculated by regression analysis as described in Materials and Methods.

determined catalytic parameters of wild type and cleavage site mutant on three different synthetic substrates (Table 1). In agreement with the positional scan, a substrate containing P4 Asp (Ac-DEVD-AFC) was the least tolerated substrate. Overall, the cleavage site mutant displayed an approximately 10 times reduced activity compared to the wild type on the substrates Ac-LEHD-AFC and Ac-IETD-AFC and about 30 times reduced activity on Ac-DEVD-AFC. As expected from our findings described above, this is consistent with an increase in catalytic potency upon autocleavage but not consistent with a switch in specificity on small peptides.

The Cleavage Site Mutant Has Restricted Specificity on Protein Substrates. While not affecting the processing of small substrates, differences in the stabilization of the active site and its surroundings might significantly affect the activity of the enzyme on large protein substrates. Therefore, we characterized the role of autocleavage of caspase-10 in a more natural context and analyzed cleavage of known protein substrates. Rates of cleavage were measured by incubating 1 μM protein substrate for 1 h at 37 °C with a dilution series of protease, preactivated in sodium citrate, followed by Western blot analysis, and kinetic rates were determined as described in the enzymes (10 nM) were incubated in 1.0 M sodium citrate for 30 min at 37 °C before measuring activity in a dilution series of the indicated substrates. Kinetic values (for three replicate data sets) were calculated by regression analysis as described in Materials and Methods. Pro-caspase-3, pro-caspase-7, and RIPK1, reported substrates for apical caspases (*23*, *38*, *50*−*52*), were readily cleaved by wild-type

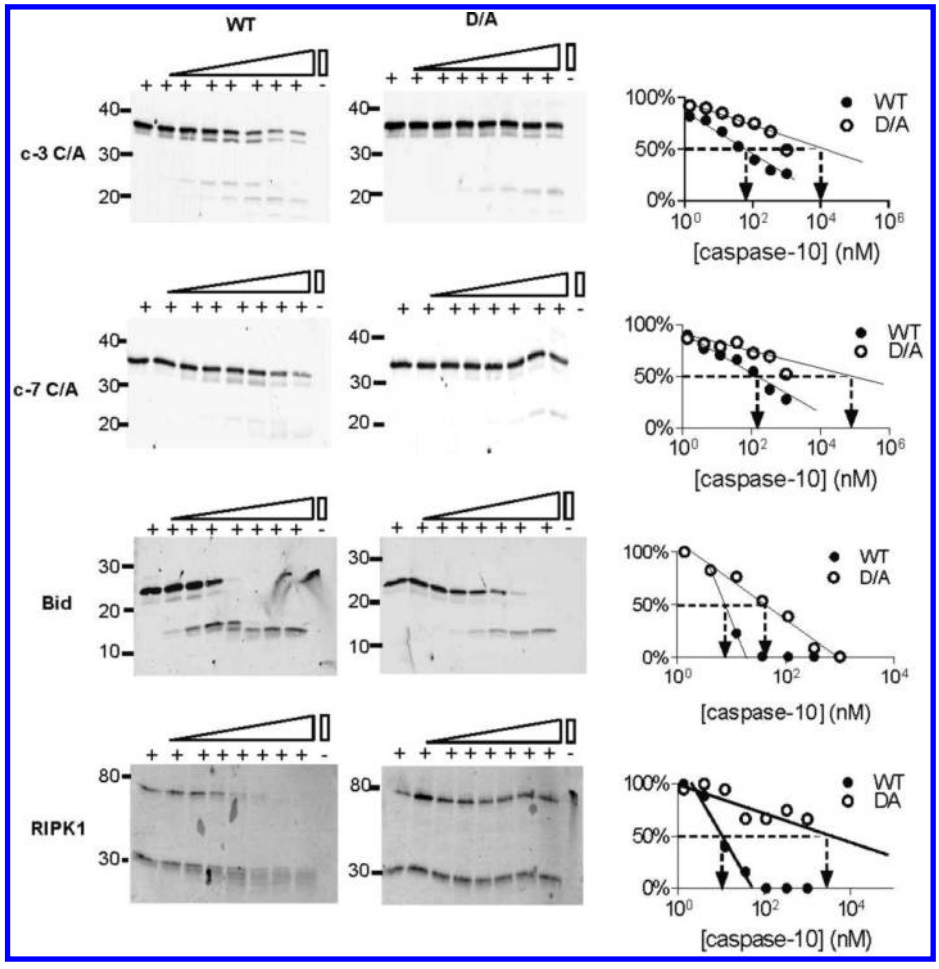

FIGURE 5: Cleavage site mutant shows restricted specificity on protein substrates. A constant amount of substrate was incubated with increasing amounts of enzyme, and disappearance of the full-length substrate was determined by quantifying the fluorescence signal of the secondary antibody with an Odyssey infrared scanner (LI-COR Biosciences). These values were then used to calculate k_{cat}/K_M as described. Protein substrates [1 μM] were incubated as indicated with a dilution series of caspase-10 wild type or cleavage site mutant (preincubated in 1 M sodium citrate buffer for 30 min at 37 °C) for 1 h at 37 °C. Kinetic values (for three replicate data sets) were calculated by regression analysis as described in Materials and Methods. The tested substrates were catalytically inactive C/A pro-caspase-3 and pro-caspase-7 (c-3 C/A; c-7 C/A) as well as Bid and RIPK1. Note that there is already some cleaved RIPK1 present in the starting material, possibly processed by endogenous caspases in the cells wherein the protein was expressed.

caspase-10. In the case of RIPK1 this result is at odds with one study that did not find cleavage of RIPK1 by caspase-10 in caspase-8-deficient Jurkat I9.2 cells (*31*). Proteolysis of these protein substrates by the cleavage site mutant was dramatically reduced, as shown in Figure 5 and Table 2. The exception is the apical caspase substrate Bid (*53*−*55*), described as the central link between the two apoptotic pathways, mediating the communication between DISCs and mitochondrial events. In this case the uncleaved form of caspase-10 processes Bid (1 μM) with a k_{cat}/K_M of 4.6×10^3 (Table 2) similar to that of the cleaved wild type. Since the uncleaved form of caspase-10 most likely exists early on in the DISCs and/or upon low level DISC formation, this finding is informative in interpreting the kinetics of sequential caspase activation and substrate utilization.

In detail Bid has two putative cleavage sites for apical caspases, LQTD/G and IEPD/S, with the second also being a reported cleavage site for granzyme B (*56*−*59*). Wild-type caspase-10 was able to process both sites, as reported before (*38*). The first cleavage appeared at the caspase site and, with increasing protease concentration, also at the granzyme B site with complete disappearance of the full-length Bid. Interestingly, the cleavage site mutant processed Bid only at the caspase site but not at the granzyme B site.

Table 2: Catalytic Parameters on Different Protein Substrates[a]

c-10	WT		D/A	
substrate	$E_{1/2}$ (nM)	k_{cat}/K_M (M^{-1} s^{-1})	$E_{1/2}$ (nM)	k_{cat}/K_M (M^{-1} s^{-1})
pro-casp-3	62	3.1×10^3	10005	19.2
pro-casp-7	144	1.3×10^3	76000	2.5
Bid	7.7	2.5×10^4	41.7	4.6×10^3
RIPK1	11.4	1.7×10^4	2898	66.4

[a]Protein substrates were incubated with increasing amounts of either caspase-10 wild type or cleavage site mutant. $E_{1/2}$ is the concentration of caspase-10 required for 50% cleavage of the substrate and was used to calculate k_{cat}/K_M.

Figure 6 shows the fractional activity of the cleavage site mutant compared to the wild type for the tested peptide and protein substrates with the cleavage sites indicated in the figure. One can see that there is a dramatic difference between pro-caspase-3, -7, RIPK1, and Bid. Comparison of the cleavage motifs with the results from the P1 library would not support this striking difference, leading to the conclusion that other factors are involved in the regulation of substrate selectivity, such as accessibility of the cleavage site or exosite interactions.

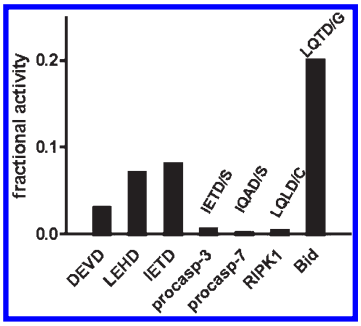

FIGURE 6: Restricted substrate specificity of the cleavage site mutant. Comparison of cleavage site mutant to wild type with respect to substrate preference (fractional activity of the cleavage site mutant with wild-type rates set as one). The cleavage sites (P4−P1′) identified in the protein substrates are indicated above the bars.

DISCUSSION

In humans, two apical caspases are implicated in triggering the extrinsic death pathway: caspase-8 and caspase-10 (*27*, *30*, *31*, *60*, *61*). Despite reports that caspase-10 is recruited to the DISC and able to initiate apoptosis (*30*, *31*), most previous research on the role of caspases in the extrinsic pathway has focused on caspase-8; indeed, there are over 20 times more citations in PubMed on caspase-8 than on caspase-10. One reason for this could be that caspase-10 is not expressed in the rodent lineage and therefore less amenable to genetic studies. However, protein sequence alignment of the two caspases shows high similarity, and even though there is not yet a crystal structure of caspase-10, one would expect a similar folding and function of the protein.

Surprisingly, the recombinant cleavage site mutant was not processed although there is a second conserved cleavage site in the linker region. This site is apparently not processed by autoproteolysis, which distinguishes caspase-10 from human caspase-8, where two sites undergo autoproteolysis (*17*) (Figure 1B). Indeed, even after full activation of the mutant in optimal kosmotrope we failed to see any cleavage, and material remained as a single chain. It is possible that the second potential cleavage site in caspase-10 is a remnant of the twin caspase-8 cleavage sites, but since the role of the twin cleavage sites in human caspase-8 is unknown, further speculation is fruitless at this point. Enzymatic activity of caspase-10 was greatly enhanced by kosmotrope-induced dimerization, although the overall activity of the mutant was significantly lower as compared to the wild type. These results agree with the hypothesis that dimerization is the activating event, whereas cleavage of the linker stabilizes the dimer, shifting the equilibrium toward a fully active enzyme, as demonstrated for caspase-8 (*16*−*20*).

To address the important caveat of using kosmotropic salts, which do not represent physiological conditions, we employed an inducible dimerization system. We show that the wild-type caspase-10 is fully activated with stoichiometric amounts of the dimerizer AP20187, whereas the cleavage site mutant had no measurable activity with AP20187 alone, even though size-exclusion chromatography confirmed that the mutant becomes dimeric in the presence of the compound. Interestingly, the positive control in sodium citrate displayed activity of the fusion proteins of both wild type and cleavage site mutant. Because simple dimerization of the cleavage site mutant failed to activate caspase-10, we considered the possibility that citrate activates the zymogen by somehow generating an active site in the monomer. However, this seems unlikely given that Fv-mediated dimerization substantially lowers the concentration of citrate required to activate caspase-10. This implies that dimerization of the Fv-domain is necessary but not sufficient to fully activate the cleavage site mutant, which serves as a model of the initial form of the caspase-10 zymogen recruited to the DISC.

The simplest explanation is that the dimerized Fv-domain is not in an optimal conformation to allow the same dimer conformation of the catalytic domain that would be driven by the native DEDs in the DISC, which the Fv-domain simulates. The Fv-mediated dimer is simply not organized precisely enough, and the Fv-mediated wild type overcomes this deficit because of additional interactions between the cleaved portions of the structure (Figure 1C). Yet, as outlined above, the consequence of this line of reasoning is that kosmotropes such as citrate promote dimerization of the monomer zymogen of caspase-10 with an additional role in stabilizing active site loops. Taken together, our data strongly suggest that caspase-10 follows the proximity-induced dimerization model for apical caspases.

It is possible that the decrease in substrate hydrolysis of the noncleavable protease is utilized *in vivo* to convey substrate preferences. To investigate this possibility, we tested the cleaved and noncleavable caspase-10 on a P1 Asp-fixed positional scanning substrate library in the presence of 1.0 M sodium citrate to provide robust activity of both proteins. The library revealed very similar subsite preferences (P4−P3−P2) for both the wild-type and mutant caspase-10. However, when we compared the catalytic parameters of the cleaved versus the noncleavable enzyme on small peptide substrates and protein substrates, there seemed to be a big difference in the efficiency of protein substrate processing. While the efficiency reflected by k_{cat}/K_M on three different peptide substrates, Ac-LEHD-AFC, Ac-IETD-AFC, and Ac-DEVD-AFC, was quite comparable, the difference on protein substrates was striking. These findings are summarized in Figure 6. The wild-type caspase-10 was able to process each protein with relatively good k_{cat}/K_M in a range from 1.3×10^3 to 2.5×10^4, with Bid and RIPK1 as the best substrates. Cleavage of the four proteins tested supports the proapoptotic function of caspase-10. Intriguingly, although the cleavage site mutant processed pro-caspase-3, pro-caspase-7, and RIPK1 very poorly, in comparison, Bid appeared to be a bona fide substrate with a k_{cat}/K_M of 4.6×10^3. The substantial difference in the activity of the cleavage site mutant on Bid vs RIPK1 despite their very similar cleavage site motifs (LQTD/G vs LQLD/G) is plausible through a different mode of presentation of these sequences. Previous work (*62*) has shown that linkers or loops and their lengths significantly influence the presentation of the cleavage motifs and thus play an important role for the efficiency by which protease substrates get processed. In Bid we find an extended long protruding loop containing the cleavage site LQTD/G, presented by a Bcl-2 fold scaffold which can serve as an appropriate basis for the near optimal behavior as a caspase substrate. If we consider that cleavage of Bid has been reported to be an exclusively prodeath signal (*53*, *54*, *63*), we come to the hypothesis that the uncleaved form of caspase-10 has a prodeath role, which is in contrast to data on the role of cleavage in caspase-8.

Noncleavable caspase-8, expressed in mouse cells, was not able to trigger apoptosis but could still perform nonapoptotic functions, such as proliferation of T-lymphocytes and B-lymphocytes or macrophage differentiation (*16*). Another approach to study the role of cleavage in caspase-8 was taken by reconstituting the DISC *in vitro*, and this has led to the conclusion that caspase-8

cleavage is necessary to induce DISC-mediated apoptosis (*18*) and that uncleaved caspase-8 has a restricted substrate repertoire that supports cell survival. Our data argue that caspase-10 does not demonstrate a specific alteration in specificity upon cleavage that would adjust its specificity toward a nondeath role, distinguishing it from caspase-8.

In conclusion, we established the activation mechanism and primary specificity of caspase-10. Our results reveal a similar activation mechanism and intrinsic substrate preference to caspase-8, though with restricted tolerance in the P4 pocket. Importantly, we observe that cleavage of the caspase allows for substantially accelerated cleavage of protein substrates, with the exception of Bid, for which caspase cleavage was not required, and which is an excellent substrate for both cleaved and uncleaved caspase-10. Though it is yet too early to support in detail, this finding tends to disagree with a potential nondeath role for uncleaved caspase-10.

ACKNOWLEDGMENT

We thank Stan Krajewski for providing the anti-Bid antibody, John C. Reed and Dayong Zhai for the Bid plasmid, Jurg Tschopp for the RIPK1 plasmid, and Mari Enoksson for helpful discussion.

REFERENCES

1. Strasser, A., O'Connor, L., and Dixit, V. M. (2000) Apoptosis signaling. *Annu. Rev. Biochem. 69*, 217–245.
2. Fuentes-Prior, P., and Salvesen, G. S. (2004) The protein structures that shape caspase activity, specificity, activation and inhibition. *Biochem. J. 384*, 201–232.
3. Budihardjo, I., Oliver, H., Lutter, M., Luo, X., and Wang, X. (1999) Biochemical pathways of caspase activation during apoptosis. *Annu. Rev. Cell Dev. Biol. 15*, 269–290.
4. Green, D. R. (1998) Apoptotic pathways: the roads to ruin. *Cell 94*, 695–698.
5. Bratton, S. B., and Cohen, G. M. (2003) Death receptors leave a caspase footprint that Smacs of XIAP. *Cell Death Differ. 10*, 4–6.
6. Salvesen, G. S., and Duckett, C. S. (2002) IAP proteins: blocking the road to death's door. *Nat. Rev. Mol. Cell Biol. 3*, 401–410.
7. Turk, B., and Stoka, V. (2007) Protease signalling in cell death: caspases versus cysteine cathepsins. *FEBS Lett. 581*, 2761–2767.
8. Scott, F. L., Stec, B., Pop, C., Dobaczewska, M. K., Lee, J. J., Monosov, E., Robinson, H., Salvesen, G. S., Schwarzenbacher, R., and Riedl, S. J. (2009) The Fas-FADD death domain complex structure unravels signalling by receptor clustering. *Nature 457*, 1019–1022.
9. Peter, M. E., and Krammer, P. H. (2003) The CD95(APO-1/Fas) DISC and beyond. *Cell Death Differ. 10*, 26–35.
10. Ashkenazi, A., and Dixit, V. M. (1998) Death receptors: signaling and modulation. *Science 281*, 1305–1308.
11. Falschlehner, C., Schaefer, U., and Walczak, H. (2009) Following TRAIL's path in the immune system. *Immunology 127*, 145–154.
12. Micheau, O., Thome, M., Schneider, P., Holler, N., Tschopp, J., Nicholson, D. W., Briand, C., and Grutter, M. G. (2002) The long form of FLIP is an activator of caspase-8 at the Fas death-inducing signaling complex. *J. Biol. Chem. 277*, 45162–45171.
13. Chang, D. W., Xing, Z., Pan, Y., Algeciras-Schimnich, A., Barnhart, B. C., Yaish-Ohad, S., Peter, M. E., and Yang, X. (2002) c-FLIP(L) is a dual function regulator for caspase-8 activation and CD95-mediated apoptosis. *EMBO J. 21*, 3704–3714.
14. Boatright, K. M., Deis, C., Denault, J. B., Sutherlin, D. P., and Salvesen, G. S. (2004) Activation of caspases-8 and -10 by FLIP(L). *Biochem. J. 382*, 651–657.
15. Boatright, K. M., Renatus, M., Scott, F. L., Sperandio, S., Shin, H., Pedersen, I. M., Ricci, J. E., Edris, W. A., Sutherlin, D. P., Green, D. R., and Salvesen, G. S. (2003) A unified model for apical caspase activation. *Mol. Cell 11*, 529–541.
16. Kang, T. B., Oh, G. S., Scandella, E., Bolinger, B., Ludewig, B., Kovalenko, A., and Wallach, D. (2008) Mutation of a self-processing site in caspase-8 compromises its apoptotic but not its nonapoptotic functions in bacterial artificial chromosome-transgenic mice. *J. Immunol. 181*, 2522–2532.
17. Chang, D. W., Xing, Z., Capacio, V. L., Peter, M. E., and Yang, X. (2003) Interdimer processing mechanism of procaspase-8 activation. *EMBO J. 22*, 4132–4142.
18. Hughes, M. A., Harper, N., Butterworth, M., Cain, K., Cohen, G. M., and MacFarlane, M. (2009) Reconstitution of the death-inducing signaling complex reveals a substrate switch that determines CD95-mediated death or survival. *Mol. Cell 35*, 265–279.
19. Oberst, A., Pop, C., Tremblay, A. G., Blais, V., Denault, J. B., Salvesen, G. S., and Green, D. R. (2010) Inducible dimerization and inducible cleavage reveal a requirement for both processes in caspase-8 activation, *J. Biol. Chem.*
20. Pop, C., Fitzgerald, P., Green, D. R., and Salvesen, G. S. (2007) Role of proteolysis in caspase-8 activation and stabilization. *Biochemistry 46*, 4398–4407.
21. Clackson, T., Yang, W., Rozamus, L. W., Hatada, M., Amara, J. F., Rollins, C. T., Stevenson, L. F., Magari, S. R., Wood, S. A., Courage, N. L., Lu, X., Cerasoli, F., Jr., Gilman, M., and Holt, D. A. (1998) Redesigning an FKBP-ligand interface to generate chemical dimerizers with novel specificity. *Proc. Natl. Acad. Sci. U.S.A. 95*, 10437–10442.
22. Xie, X., Zhao, X., Liu, Y., Zhang, J., Matusik, R. J., Slawin, K. M., and Spencer, D. M. (2001) Adenovirus-mediated tissue-targeted expression of a caspase-9-based artificial death switch for the treatment of prostate cancer. *Cancer Res. 61*, 6795–6804.
23. Fernandes-Alnemri, T., Armstrong, R. C., Krebs, J., Srinivasula, S. M., Wang, L., Bullrich, F., Fritz, L. C., Trapani, J. A., Tomaselli, K. J., Litwack, G., and Alnemri, E. S. (1996) In vitro activation of CPP32 and Mch3 by Mch4, a novel human apoptotic cysteine protease containing two FADD-like domains. *Proc. Natl. Acad. Sci. U.S.A. 93*, 7464–7469.
24. Grenet, J., Teitz, T., Wei, T., Valentine, V., and Kidd, V. J. (1999) Structure and chromosome localization of the human CASP8 gene. *Gene 226*, 225–232.
25. Kischkel, F. C., Kioschis, P., Weitz, S., Poustka, A., Lichter, P., and Krammer, P. H. (1998) Assignment of CASP8 to human chromosome band 2q33→q34 and Casp8 to the murine syntenic region on chromosome 1B-proximal C by in situ hybridization. *Cytogenet. Cell Genet. 82*, 95–96.
26. Goepel, F., Weinmann, P., Schymeinsky, J., and Walzog, B. (2004) Identification of caspase-10 in human neutrophils and its role in spontaneous apoptosis. *J. Leukocyte Biol. 75*, 836–843.
27. Sprick, M. R., Rieser, E., Stahl, H., Grosse-Wilde, A., Weigand, M. A., and Walczak, H. (2002) Caspase-10 is recruited to and activated at the native TRAIL and CD95 death-inducing signalling complexes in a FADD-dependent manner but can not functionally substitute caspase-8. *EMBO J. 21*, 4520–4530.
28. Wang, H., Wang, P., Sun, X., Luo, Y., Wang, X., Ma, D., and Wu, J. (2007) Cloning and characterization of a novel caspase-10 isoform that activates NF-kappa B activity. *Biochim. Biophys. Acta 1770*, 1528–1537.
29. Ng, P. W., Porter, A. G., and Janicke, R. U. (1999) Molecular cloning and characterization of two novel pro-apoptotic isoforms of caspase-10. *J. Biol. Chem. 274*, 10301–10308.
30. Kischkel, F. C., Lawrence, D. A., Tinel, A., LeBlanc, H., Virmani, A., Schow, P., Gazdar, A., Blenis, J., Arnott, D., and Ashkenazi, A. (2001) Death receptor recruitment of endogenous caspase-10 and apoptosis initiation in the absence of caspase-8. *J. Biol. Chem. 276*, 46639–46646.
31. Wang, J., Chun, H. J., Wong, W., Spencer, D. M., and Lenardo, M. J. (2001) Caspase-10 is an initiator caspase in death receptor signaling. *Proc. Natl. Acad. Sci. U.S.A. 98*, 13884–13888.
32. Wang, J., Zheng, L., Lobito, A., Chan, F. K., Dale, J., Sneller, M., Yao, X., Puck, J. M., Straus, S. E., and Lenardo, M. J. (1999) Inherited human caspase 10 mutations underlie defective lymphocyte and dendritic cell apoptosis in autoimmune lymphoproliferative syndrome type II. *Cell 98*, 47–58.
33. Worth, A., Thrasher, A. J., and Gaspar, H. B. (2006) Autoimmune lymphoproliferative syndrome: molecular basis of disease and clinical phenotype. *Br. J. Haematol. 133*, 124–140.
34. Filomenko, R., Prevotat, L., Rebe, C., Cortier, M., Jeannin, J. F., Solary, E., and Bettaieb, A. (2006) Caspase-10 involvement in cytotoxic drug-induced apoptosis of tumor cells. *Oncogene 25*, 7635–7645.
35. Lee, H. J., Pyo, J. O., Oh, Y., Kim, H. J., Hong, S. H., Jeon, Y. J., Kim, H., Cho, D. H., Woo, H. N., Song, S., Nam, J. H., Kim, H. J., Kim, K. S., and Jung, Y. K. (2007) AK2 activates a novel apoptotic pathway through formation of a complex with FADD and caspase-10. *Nat. Cell Biol. 9*, 1303–1310.
36. Park, S. J., Wu, C. H., Gordon, J. D., Zhong, X., Emami, A., and Safa, A. R. (2004) Taxol induces caspase-10-dependent apoptosis. *J. Biol. Chem. 279*, 51057–51067.

37. Bae, S., Ha, T. S., Yoon, Y., Lee, J., Cha, H. J., Yoo, H., Choe, T. B., Li, S., Sohn, I., Kim, J. Y., Kim, C. S., Jin, H. O., Lee, H. C., Park, I. C., Kim, C. S., Jin, Y. W., and Ahn, S. K. (2008) Genome-wide screening and identification of novel proteolytic cleavage targets of caspase-8 and -10 in vitro. *Int. J. Mol. Med. 21*, 381–386.
38. Fischer, U., Stroh, C., and Schulze-Osthoff, K. (2006) Unique and overlapping substrate specificities of caspase-8 and caspase-10. *Oncogene 25*, 152–159.
39. Chen, H., Xia, Y., Fang, D., Hawke, D., and Lu, Z. (2009) Caspase-10-mediated heat shock protein 90 beta cleavage promotes UVB irradiation-induced cell apoptosis. *Mol. Cell. Biol. 29*, 3657–3664.
40. Benkova, B., Lozanov, V., Ivanov, I. P., and Mitev, V. (2009) Evaluation of recombinant caspase specificity by competitive substrates. *Anal. Biochem. 394*, 68–74.
41. Stennicke, H. R., and Salvesen, G. S. (1999) Caspases: preparation and characterization. *Methods 17*, 313–319.
42. Stennicke, H. R., and Salvesen, G. S. (2000) Caspase assays. *Methods Enzymol. 322*, 91–100.
43. Scott, F. L., Fuchs, G. J., Boyd, S. E., Denault, J. B., Hawkins, C. J., Dequiedt, F., and Salvesen, G. S. (2008) Caspase-8 cleaves histone deacetylase 7 and abolishes its transcription repressor function. *J. Biol. Chem. 283*, 19499–19510.
44. Keller, N., Mares, J., Zerbe, O., and Grutter, M. G. (2009) Structural and biochemical studies on procaspase-8: new insights on initiator caspase activation. *Structure 17*, 438–448.
45. Eswar, N., Webb, B., Marti-Renom, M. A., Madhusudhan, M. S., Eramian, D., Shen, M. Y., Pieper, U., Sali, A. (2006) Comparative protein structure modeling using Modeller, *Curr. Protoc. Bioinf.* Chapter 5, Unit.
46. Walters, J., Pop, C., Scott, F. L., Drag, M., Swartz, P., Mattos, C., Salvesen, G. S., and Clark, A. C. (2009) A constitutively active and uninhibitable caspase-3 zymogen efficiently induces apoptosis. *Biochem. J. 424*, 335–345.
47. Barbero, S., Barila, D., Mielgo, A., Stagni, V., Clair, K., and Stupack, D. (2008) Identification of a critical tyrosine residue in caspase 8 that promotes cell migration. *J. Biol. Chem. 283*, 13031–13034.
48. Schmidt, U., and Darke, P. L. (1997) Dimerization and activation of the herpes simplex virus type 1 protease. *J. Biol. Chem. 272*, 7732–7735.
49. Thornberry, N. A., Rano, T. A., Peterson, E. P., Rasper, D. M., Timkey, T., Garcia-Calvo, M., Houtzager, V. M., Nordstrom, P. A., Roy, S., Vaillancourt, J. P., Chapman, K. T., and Nicholson, D. W. (1997) A combinatorial approach defines specificities of members of the caspase family and granzyme B. Functional relationships established for key mediators of apoptosis. *J. Biol. Chem. 272*, 17907–17911.
50. Van de Craen, M., Declercq, W., Van, d. b., I., Fiers, W., and Vandenabeele, P. (1999) The proteolytic procaspase activation network: an in vitro analysis. *Cell Death Differ. 6*, 1117–1124.
51. Lin, Y., Devin, A., Rodriguez, Y., and Liu, Z. G. (1999) Cleavage of the death domain kinase RIP by caspase-8 prompts TNF-induced apoptosis. *Genes Dev. 13*, 2514–2526.
52. Martinon, F., Holler, N., Richard, C., and Tschopp, J. (2000) Activation of a pro-apoptotic amplification loop through inhibition of NF-kappaB-dependent survival signals by caspase-mediated inactivation of RIP. *FEBS Lett. 468*, 134–136.
53. Li, H., Zhu, H., Xu, C. J., and Yuan, J. (1998) Cleavage of BID by caspase 8 mediates the mitochondrial damage in the Fas pathway of apoptosis. *Cell 94*, 491–501.
54. Luo, X., Budihardjo, I., Zou, H., Slaughter, C., and Wang, X. (1998) Bid, a Bcl2 interacting protein, mediates cytochrome *c* release from mitochondria in response to activation of cell surface death receptors. *Cell 94*, 481–490.
55. Milhas, D., Cuvillier, O., Therville, N., Clave, P., Thomsen, M., Levade, T., Benoist, H., and Segui, B. (2005) Caspase-10 triggers Bid cleavage and caspase cascade activation in FasL-induced apoptosis. *J. Biol. Chem. 280*, 19836–19842.
56. Alimonti, J. B., Shi, L., Baijal, P. K., and Greenberg, A. H. (2001) Granzyme B induces BID-mediated cytochrome *c* release and mitochondrial permeability transition. *J. Biol. Chem. 276*, 6974–6982.
57. Heibein, J. A., Goping, I. S., Barry, M., Pinkoski, M. J., Shore, G. C., Green, D. R., and Bleackley, R. C. (2000) Granzyme B-mediated cytochrome *c* release is regulated by the Bcl-2 family members bid and Bax. *J. Exp. Med. 192*, 1391–1402.
58. Pinkoski, M. J., Waterhouse, N. J., Heibein, J. A., Wolf, B. B., Kuwana, T., Goldstein, J. C., Newmeyer, D. D., Bleackley, R. C., and Green, D. R. (2001) Granzyme B-mediated apoptosis proceeds predominantly through a Bcl-2-inhibitable mitochondrial pathway. *J. Biol. Chem. 276*, 12060–12067.
59. Sutton, V. R., Davis, J. E., Cancilla, M., Johnstone, R. W., Ruefli, A. A., Sedelies, K., Browne, K. A., and Trapani, J. A. (2000) Initiation of apoptosis by granzyme B requires direct cleavage of bid, but not direct granzyme B-mediated caspase activation. *J. Exp. Med. 192*, 1403–1414.
60. Boldin, M. P., Goncharov, T. M., Goltsev, Y. V., and Wallach, D. (1996) Involvement of MACH, a novel MORT1/FADD-interacting protease, in Fas/APO-1- and TNF receptor-induced cell death. *Cell 85*, 803–815.
61. Muzio, M., Chinnaiyan, A. M., Kischkel, F. C., O'Rourke, K., Shevchenko, A., Ni, J., Scaffidi, C., Bretz, J. D., Zhang, M., Gentz, R., Mann, M., Krammer, P. H., Peter, M. E., and Dixit, V. M. (1996) FLICE, a novel FADD-homologous ICE/CED-3-like protease, is recruited to the CD95 (Fas/APO-1) death-inducing signaling complex. *Cell 85*, 817–827.
62. Timmer, J. C., Zhu, W., Pop, C., Regan, T., Snipas, S. J., Eroshkin, A. M., Riedl, S. J., and Salvesen, G. S. (2009) Structural and kinetic determinants of protease substrates. *Nat. Struct. Mol. Biol. 16*, 1101–1108.
63. Gross, A., Yin, X. M., Wang, K., Wei, M. C., Jockel, J., Milliman, C., Erdjument-Bromage, H., Tempst, P., and Korsmeyer, S. J. (1999) Caspase cleaved BID targets mitochondria and is required for cytochrome *c* release, while BCL-XL prevents this release but not tumor necrosis factor-R1/Fas death. *J. Biol. Chem. 274*, 1156–1163.